Structure and Redox Chemistry of Analogous Nickel Thiolato and Selenolato Complexes: Implications for the Nickel Sites in Hydrogenases

Suranjan B. Choudhury, Michelle A. Pressler, Shaukat A. Mirza, Roberta O. Day, and Michael J. Maroney*

Department of Chemistry, University of Massachusetts, Amherst, Massachusetts 01003

Received January 21, 1994[⊗]

The syntheses, structures, and redox properties of isomorphous Ni(II) thiolato and selenolato complexes of the tridentate ligands bis(2-(hydrochalcogeno)ethyl)methylamines are reported. Reaction of $Ni(OAc)_2$ with bis(2-mercaptoethyl)methylamine leads to the formation of a dimeric complex, bis{[(μ-2-mercaptoethyl)(2-mercaptoethyl)-methylaminato(2−)]nickel(II)}, $[Ni(\mathbf{1})]_2$. This complex contains planar, diamagnetic Ni(II) centers ligated by a tertiary amine N-donor atom, a terminal thiolate, and two thiolates that bridge to the second Ni center in the dimer. Crystals of $[Ni(\mathbf{1})]_2$ form in orthorhombic space group $Pna2_1$ with cell dimensions $a = 19.695(2)$ Å, $b = 6.042(2)$ Å, $c = 13.463(3)$ Å, $V = 1602(1)$ Å^3, and $Z = 4$. Reaction of $Ni(OAc)_2$ with bis(2-(hydroseleno)-ethyl)methylamine results in the formation of a structurally analogous dimeric complex, bis{[(μ-2-(hydroseleno)-ethyl)(2-(hydroseleno)ethyl)methylaminato(2−)]nickel(II)}, $[Ni(\mathbf{2})]_2$, where all of the chalcogenolate donors are selenolates. Crystals of $[Ni(\mathbf{2})]_2$ are isomorphous with those of $[Ni(\mathbf{1})]_2$, with $a = 20.040(8)$ Å, $b = 6.265(2)$ Å, $c = 13.590(5)$ Å, and $V = 1706(2)$ Å^3. One-electron oxidation of either dimeric complex leads to the formation of radical cations, which exhibit EPR spectra consistent with $S = {}^1/_2$ radicals. For $[Ni(\mathbf{1})]_2^+$ the g values observed ($g_x = 2.20$, $g_y = 2.14$, $g_z = 2.02$) are essentially identical to those observed for a reduced and catalytically viable redox state of Fe,Ni hydrogenases ($g_x = 2.20$, $g_y = 2.14$, $g_z = 2.01$). The substitution of Se- for S-donors in $[Ni(\mathbf{2})]_2$ does not alter the observed g values much ($g_x = 2.23$, $g_y = 2.14$, $g_z = 2.05$) but leads to the observation of ^{77}Se hyperfine coupling ($A_z = 129$ G) that indicates that the molecular orbital containing the unpaired spin is largely Se in character (54%). Reaction of either dimeric complex with CN^- leads to the formation of mononuclear *trans*-dichalcogenolate complexes, $[Ni(\mathbf{1})CN]^-$ and $[Ni(\mathbf{2})CN]^-$. Exposure of $[Ni(\mathbf{1})CN]^-$ to O_2 leads to the quantitative formation of a monosulfinato complex. In contrast, the selenolato complex does not react with O_2 under the same conditions. The role of selenocysteinate ligation in Fe,Ni,Se hydrogenases is discussed in view of this chemistry.

Hydrogenases (H_2ases) are metalloenzymes that catalyze the reversible two-electron oxidation of dihydrogen.[1−4] These enzymes may be grouped into three classifications on the basis of their inorganic content.[5] With one exception,[6] all H_2ases contain Fe,S clusters and the first class, the Fe-only enzymes, contain exclusively Fe and S^{2-} as inorganic constituents. The most common class of H_2ase contains Ni in addition to Fe and S^{2-} (Fe,Ni). The third class of H_2ase contains Ni, Fe, S, and Se (Fe,Ni,Se). The enzyme isolated from *Desulfovibrio baculatus* is representative of the Fe,Ni,Se enzymes.[5,7] In this enzyme, the Se atom is present as a single selenocysteine residue, which has been shown by X-ray absorption spectroscopy[8] and EPR studies[9] to be a Ni ligand donor atom. The selenocysteine residue is encoded by an internal TGA codon in the DNA sequence from *D. baculatus* and represents a conservative replacement for a cysteine residue found in the amino acid sequences of the Fe,Ni class of H_2ases.[10]

The three classes of H_2ases have been shown to be immunochemically and biochemically distinct.[11,12] Among the biochemical distinctions are differing rates of H_2 oxidation and evolution and widely differing sensitivities to deactivation by O_2.[5] The Fe-only enzymes have very high rates of both H_2 evolution ($V_m \approx 6000$ (μmol/min)/mg) and H_2 oxidation ($V_m \approx 20\,000$ (μmol/min)/mg) and are frequently referred to as bidirectional H_2ases. Fe-only H_2ases are also rapidly ($t_{1/2}$ values of minutes in air) and *irreversibly* inactivated by exposure to O_2. The Fe,Ni enzymes have activities that are typically <10% of those exhibited by Fe-only H_2ases [$V_m(H_2$ evolution) ≈ 450 (μmol/min)/mg; $V_m(H_2$ oxidation) ≈ 1500 (μmol/min)/mg] but are much more oxygen tolerant ($t_{1/2}$ values vary from hours to days) and the oxidative deactivation is *reversible*. Thus, this class of enzymes is typically isolated in air and reductively reactivated. When Se is present in H_2ase, the catalytic activities

[⊗] Abstract published in *Advance ACS Abstracts,* September 15, 1994.

(1) Adams, M. W. W. *Biochim. Biophys. Acta* **1990**, *1020*, 115−45.
(2) Cammack, R.; Fernandez, V. M.; Schneider, K. In *The Bioinorganic Chemistry of Nickel*; Lancaster, J. R., Jr., Ed.; VCH: New York, 1988; pp 167−90.
(3) Moura, J. J. G.; Teixeira, M.; Moura, I.; LeGall, J. In *The Bioinorganic Chemistry of Nickel*; Lancaster, J. R., Jr., Ed.; VCH: New York, 1988; pp 191−226.
(4) Przybyla, A. E.; Robbins, J.; Menon, N.; Peck, H. D. J. *FEMS Microbiol. Rev.* **1992**, *88*, 109−35.
(5) Fauque, G.; Peck, H. D., Jr.; Moura, J. J. G.; Huynh, B. H.; Berlier, Y.; DerVartanian, D. V.; Teixeira, M.; Przybyla, A. E.; Lespinat, P. A.; Moura, I.; LeGall, J. *FEMS Microbiol. Rev.* **1988**, *54*, 299−344.
(6) Zirngibl, C.; Van Dongen, W.; Schworer, B.; Von Bunau, R.; Richter, M.; Klein, A.; Thauer, R. K. *Eur. J. Biochem.* **1992**, *208*, 511−20.
(7) Teixeira, M.; Fauque, G.; Moura, I.; Lespinat, P. A.; Berlier, Y.; Prickril, B.; Peck, H. J.; Xavier, A. V.; LeGall, J.; Moura, J. J. *Eur. J. Biochem.* **1987**, *167*, 47−58.
(8) Eidsness, M. K.; Scott, R. A.; Prickril, B. C.; DerVartanian, D. V.; Legall, J.; Moura, I.; Moura, J. J. G.; Peck, H. J. *Proc. Natl. Acad. Sci. U.S.A.* **1989**, *86*, 147−51.
(9) He, S. H.; Teixeira, M.; LeGall, J.; Patil, D. S.; Moura, I.; Moura, J. J. G.; DerVartanian, D. V.; Huynh, B. H.; Peck, H. D., Jr. *J. Biol. Chem.* **1989**, *264*, 2678−82.
(10) Voordouw, G.; Menon, N. K.; LeGall, J.; Choi, E. S.; Peck, H. J.; Przybyla, A. E. *J. Bacteriol.* **1989**, *171*, 2894−9.
(11) Kovacs, K. L.; Seefeldt, L. C.; Tigyi, G.; Doyle, C. M.; Mortenson, L. E.; Arp, D. J. *J.Bacteriol.* **1989**, *171*, 430−5.
(12) Lorenz, B.; Schneider, K.; Kratzin, H.; Schlegel, H. G. *Biochim. Biophys. Acta* **1989**, *995*, 1−9.

0020-1669/94/1333-4831$04.50/0

are generally less than observed in Fe,Ni enzymes [$V_m(H_2$ evolution) $\approx$ 450 (μmol/min)/mg; $V_m(H_2$ oxidation) $\approx$ 100 (μmol/min)/mg] but the Fe,Ni,Se enzymes may be isolated in air in a form that does not require reductive activation.[5] In general, the decrease in H_2 oxidation activity is paralleled by increasing affinity for H_2 and higher H_2/HD ratios in proton–deuteron exchange assays.

The contrast in O_2 sensitivity, H_2 oxidation activity, and H/D exchange activity between the Fe,Ni and Fe,Ni,Se H_2ases suggests that the modification of the Ni site by the inclusion of a selenocysteinate ligand is responsible for the biochemical differences. In order to address the effects of selenolate ligation on the redox chemistry of the Ni site, we have synthesized and characterized two structurally analogous dimeric complexes of tridentate bis(2-(hydrochalcogeno)ethyl)methylamine ligands: one containing alkanethiolate donors similar to the cysteinate ligands found in Fe,Ni H_2ases and one containing selenolate ligands that mimic coordination of Ni by selenocysteine. The crystal structures of these two compounds reveal that they constitute a rare example of isomorphous thiolate and selenolate complexes, and the comparison of the structures of these two compounds, their redox properties, and the redox properties of their mononuclear cyanide adducts provides chemical insights into the role of Se in the Fe,Ni,Se hydrogenases.

Experimental Section

Synthesis. All solvents were dried by using conventional methods and distilled and stored under N_2 atmosphere. Except where noted, starting materials were of reagent grade and were obtained from the commercial sources indicated. All synthetic procedures involving manipulations of solutions of the ligands and their Ni complexes were carried out under an N_2 atmosphere by using standard Schlenk techniques unless otherwise noted. Samples submitted for microanalysis were routinely ground to a fine powder and vacuum-desiccated over P_4O_{10} overnight prior to analysis.

Bis(2-mercaptoethyl)methylamine Hydrochloride. This ligand was prepared and purified as previously described.[13]

Bis{[(μ-2-mercaptoethyl)(2-mercaptoethyl)methylaminato(2−)]-nickel(II)}, [Ni(1)]$_2$. This complex was prepared as previously described.[13] The crystals used for the single-crystal X-ray diffraction structure determination were obtained by slow diffusion (3–4 days) of a layer of ether (5 mL) into a solution of [Ni(**1**)]$_2$ (10 mg) in a minimum amount of dimethylformamide.

Tetraethylammonium *trans*-[Bis(2-mercaptoethyl)methylaminato(2−)](cyanato)nickelate, Et$_4$N[Ni(1)CN]. This complex was synthesized from [Ni(**1**)]$_2$ by the addition of Et$_4$N(CN) (Fluka) as previously described.[13]

Bis(2-(hydroseleno)ethyl)methylamine. Bis(2-chloroethyl)methylamine hydrochloride (Aldrich) (5.34 g, 27.8 mmol) was dissolved in methanol (30 mL). To this solution was added dry Et_3N (2.80 g, 27.8 mmol). This solution was added gradually to a vigorously stirred solution of KSeCN (97%, Aldrich) (8.01 g, 55.6 mmol) in methanol (60 mL) that was warmed to 35 °C. The mixture was stirred at 35 °C overnight, during which time a white precipitate appeared. The precipitate was removed by filtration, and the filtrate was concentrated to 40 mL under reduced pressure. The solution was then cooled to 20 °C and was treated with $NaBH_4$ (Fisher) (2.50 g, 66.0 mmol). This mixture was stirred for 1 h and then filtered to remove any undissolved material, the filtrate was neutralized with dilute acetic acid (1:1 HOAc in methanol), and the resulting solution was used directly in the preparation of the Ni complex.

Bis{[(μ-2-(hydroseleno)ethyl)(2-(hydroseleno)ethyl)methylaminato-(2−)]nickel(II)}, [Ni(2)]$_2$. Anhydrous Ni(OAc)$_2$ (4.91 g, 27.8 mmol) was dissolved in methanol (100 mL). The solution of bis(2-(hydroseleno)ethyl)methylamine described above was added gradually to this solution, resulting in the formation of a dark green solution and a brown precipitate. The mixture was stirred for 1 h. The solvent was then removed under reduced pressure, and the solid was extracted with benzene (10 × 25 mL). The diamagnetic product was obtained as a microcrystalline solid from the benzene extract by concentration under reduced pressure. Yield = 3.2 g (38%). Anal. Calcd for $Ni_2C_{10}H_{22}N_2Se_4$: C, 19.89; H, 3.64; N, 4.64. Found: C, 20.43; H, 3.55; N, 4.46. ^{77}Se-NMR: δ = 204 ppm, δ = −28 ppm. IR (cm^{-1}) in KBr: 2910 w, 2860 w, 2830 w, 1470 m, 1450 s, 1440 s, 1420 s, 1410 s, 1345 w, 1310 s, 1260 m, 1220 s, 1200 m, 1170 m, 1135 w, 1050 m, 1030 s, 960 w, 950 w, 910 s, 880 s, 830 s, 750 s, 570 w, 520 m, 460 w.

The crystals used for the single-crystal X-ray diffraction structure determination were obtained via slow diffusion of a layer of *n*-hexane (20 mL) into a solution of [Ni(**2**)]$_2$ (100 mg) in CH_2Cl_2 (5 mL) at ambient temperature. Dark green crystals were obtained in about 2 weeks.

Tetraethylammonium *trans*-[Bis(2-(hydroseleno)ethyl)methylaminato(2−)](cyanato)nickelate, Et$_4$N[Ni(2)CN]. A solution of Et$_4$N(CN) (Fluka) (62.5 mg, 0.4 mmol) in acetonitrile (2 mL) was added to a solution of [Ni(**2**)]$_2$ (120.6 mg, 0.2 mmol) in acetonitrile (20 mL), resulting in a green solution that was stirred for $^1/_2$ h prior to the removal of the solvent under reduced pressure. The resulting diamagnetic green solid was redissolved in acetonitrile (5 mL) and precipitated by the addition of ether. The microcrystalline product was collected by filtration, washed with ether, and dried under vacuum over P_4O_{10}. Yield = 118 mg (90%). Anal. Calcd for $NiC_{14}H_{31}N_3Se_2$: C, 36.70; H, 6.82; N, 9.17. Found: C, 36.99; H, 6.71; N, 9.07. ^{77}Se-NMR: δ = 150 ppm. IR (cm^{-1}) in KBr: 2950 w, 2840 w, 2090 s (ν_{CN}), 1485 s, 1435 m, 1390 m, 1365 m, 1310 m, 1260 w, 1220 s, 1175 s, 1160 s, 1050 w, 1030 m, 1020 w, 1000 s, 910 m, 880 m, 840 m, 780 s, 765 s, 610 w, 520 w, 450 s.

Crystallography. All X-ray crystallographic studies were done using an Enraf-Nonius CAD4 diffractometer and graphite-monochromated molybdenum radiation. Details of the experimental procedures have been described previously.[14]

Crystals were mounted in thin-walled glass capillaries which were sealed as a precaution against moisture sensitivity. Data were collected using the θ–2θ scan mode with $3° \le 2\theta_{Mo\ K\bar{\alpha}} \le 43°$. Empirical absorption corrections based on ψ scans were applied (relative transmission factors on I from 0.6386 to 0.9941 for [Ni(**1**)]$_2$ and from 0.4641 to 0.9872 for [Ni(**2**)]$_2$).

The structures were solved by use of direct methods and difference Fourier techniques and were refined by full-matrix least-squares procedures.[15] All computations were performed on a MicroVax II computer using the Enraf-Nonius SDP system of programs. Crystallographic data are summarized in Table 1.

The crystal used for the study of [Ni(**1**)]$_2$ was a small lath with dimensions of 0.12 × 0.12 × 0.30 mm^3. A total of 968 independent reflections ($+h,+k,+l$) were measured. The Ni, S, and N atoms were refined anisotropically. Carbon atoms were refined isotropically.

Table 1. Crystallographic Data for [Ni(**1**)]$_2$ and [Ni(**2**)]$_2$

	[Ni(**1**)]$_2$	[Ni(**2**)]$_2$
formula	$C_{10}H_{22}N_2S_4Ni_2$	$C_{10}H_{22}N_2Se_4Ni_2$
fw	415.976	603.560
crystal system	orthorhombic	orthorhombic
space group	$Pna2_1$ (No. 33)	$Pna2_1$ (No. 33)
a (Å)	19.695(2)	20.040(8)
b (Å)	6.042(2)	6.265(2)
c (Å)	13.463(3)	13.590(5)
V (Å^3)	1602(1)	1706(2)
Z	4	4
T (°C)	23 ± 2	23 ± 2
λ (Å)	0.710 73	0.710 73
D_{calc} (g/cm^3)	1.725	2.349
μ (cm^{-1})	28.501	106.567
$R(F_o)^a$	0.034	0.059
$R_w(F_o)^a$	0.043	0.070

^{a} $R = \sum||F_o| - |F_c||/\sum|F_o|$; $R_w = [\sum w(|F_o| - |F_c|)^2/\sum w|F_o|^2]^{1/2}$.

(13) Mirza, S. A.; Pressler, M. A.; Kumar, M.; Day, R. O.; Maroney, M. J. *Inorg. Chem.* **1993**, *32*, 977–87.

(14) Sau, A. C.; Day, R. O.; Holmes, R. R. *Inorg. Chem.* **1981**, *20*, 3076–81.

(15) The function minimized was $\sum w(|F_o| - |F_c|)^2$, $w^{1/2} = 2F_oLp/\sigma_I$.

Hydrogen atoms were included in the refinement as fixed isotropic scatterers in ideal positions. The final refinement was based on 632 observed reflections ($I \geq 3\sigma_I$).

Only crystals of poor quality (broad peaks) could be obtained for $[Ni(\mathbf{2})]_2$. The crystal used for the study was cut from a defective square plate and had approximate dimensions of 0.20 × 0.35 × 0.43 mm^3. A total of 1036 independent reflections ($+h,+k,+l$) were measured. The Ni and Se atoms were refined anisotropically. The N and C atoms were refined isotropically. Hydrogen atoms were treated as described for $[Ni(\mathbf{1})]_2$. The final refinement was based on 665 observed reflections ($I \geq 3\sigma_I$).

Physical Measurements. A study of the reactivity of $Et_4N[Ni(\mathbf{1})CN]$ with O_2 and measurement of the kinetic properties of the reaction monitored by electronic absorption spectroscopy have been previously reported.[13] These experiments were repeated under identical conditions for $Et_4N[Ni(\mathbf{2})CN]$. Electronic absorption spectra were recorded by using an OLIS 4300 spectrophotometer.

Infrared spectra for routine characterization were obtained as KBr pellets on a Perkin-Elmer 783 IR spectrophotometer and calibrated with polystyrene. Relative intensities of the bands reported are indicated (w = weak, m = medium, s = strong, vs = very strong, br = broad), and assignments are indicated when they can be made with confidence.

^{77}Se-NMR spectra were recorded on $CDCl_3$ solutions of the selenolate complexes at 57.246 MHz by using a Bruker MSL-300 spectrometer and referenced to dimethyl diselenide using external diphenyl diselenide in the same solvent (δ = 460 ppm).[16]

Microanalyses were performed by the University of Massachusetts Microanalysis Laboratory.

Cyclic voltammetric and coulometric measurements and controlled-potential electrolyses were performed by using a BAS 100 electrochemistry system and *ca.* 1 mM solutions of $[Ni(\mathbf{1})]_2$ and $[Ni(\mathbf{2})]_2$ dissolved in 0.1 M n-$Bu_4N(ClO_4)$ (electrometric grade, Southwestern Analytical Chemicals)/CH_2Cl_2 solution. For cyclic voltammetry, sample solutions prepared under N_2 were transferred via syringe to a cell that was purged by a stream of CH_2Cl_2-saturated Ar. The cell contained a Pt button working electrode, a Pt wire auxiliary electrode, and a Ag wire pseudoreference electrode. The potentials obtained at a scan rate of 250 mV/s with this cell were referenced to the ferrocene/ferrocenium couple measured under identical conditions. A potential of + 400 mV vs NHE for this couple was used to convert the measured potentials to the NHE reference.[17]

Coulometric measurements and controlled-potential electrolyses were conducted at a Pt gauze working electrode in a standard H-cell that separated the working and auxiliary electrodes from the reference electrode with a sintered glass frit. The cell was cooled to *ca.* −35 °C for $[Ni(\mathbf{1})]_2$ and to −45° for $[Ni(\mathbf{2})]_2$ by using an ethanol bath cooled with liquid N_2. Oxidation was judged to be complete when the current was ≤2% of the initial current.

Oxidized samples of $[Ni(\mathbf{1})]_2$ used for EPR spectral studies were produced at −35 °C via controlled-potential electrolysis of an 0.8 mM solution of dimer in 0.1 M n-$Bu_4N(ClO_4)/CH_2Cl_2$ solutions at +650 mV vs NHE. The one-electron-oxidation product of $[Ni(\mathbf{1})]_2$ is thermally unstable and decays to an EPR-silent product even at −35 °C. To maximize the EPR signal, electrolysis was allowed to proceed until 0.7 electron/dimer had been passed. The resulting solution was transferred to an EPR tube at −35 °C and frozen by immersion in liquid N_2. The one-electron-oxidation product of $[Ni(\mathbf{2})]_2$ proved to be too unstable to produce in quantity by controlled-potential electrolysis. Attempts to do so led to the formation of a film on the working electrode and solutions that gave no observable EPR signal. Therefore, samples of the oxidation product of $[Ni(\mathbf{2})]_2$ were produced by chemical oxidation using $NOBF_4$ as an oxidant. A solution of $[Ni(\mathbf{2})]_2$ (25 mg, 0.041 mmol) was dissolved in CH_2Cl_2 (2 mL), and the resulting solution was cooled to −70 °C by using a dry ice/2-propanol bath. A solution of $NOBF_4$ (Aldrich) (5 mg, 0.043 mmol) in acetonitrile (0.5 mL) was added. The solution was stirred for $^1/_2$ h at −70 °C and was then transferred into an EPR tube at −70 °C.

(16) O'Brien, D. H.; Dereu, N.; Huang, C.-K.; Irgolic, K. J. *Organometallics* **1983**, *2*, 305−7.
(17) Gagne, R. R.; Allison, J. L.; Gall, R. S.; Koval, C. A. *J. Am. Chem. Soc.* **1977**, *99*, 1770−8.

Scheme 1

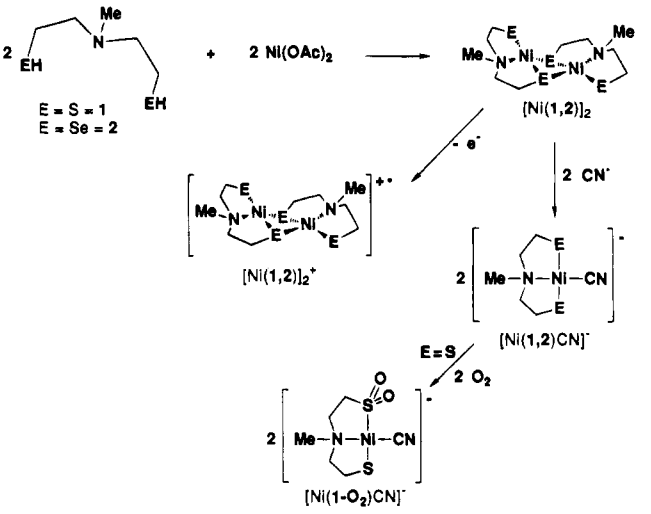

X-Band EPR spectra were recorded at 77 K on an IBM Instruments ESP-300 spectrometer by using a quartz finger dewar. Simulations of EPR spectra were performed with the NEWSIM software package (Graham George, Stanford Linear Accelerator Laboratory) on a VAX computer running the Open VMS operating system.

Magnetic measurements were made at room temperature by using a Johnson-Matthey susceptibility balance.

Results

Synthesis and Structure. The Ni complexes were synthesized by addition of $Ni(OAc)_2$ to solutions of the tridentate bis(2-(hydrochalcogeno)ethyl)methylamine ligands, leading to the formation of neutral dimeric complexes, bis{[(μ-2-mercaptoethyl)(2-mercaptoethyl)methylaminato(2−)]nickel(II)}, $[Ni(\mathbf{1})]_2$, and bis{[(μ-2-(hydroseleno)ethyl)(2-(hydroseleno)ethyl)methylaminato(2−)]nickel(II)}, $[Ni(\mathbf{2})]_2$. These dimers may be cleaved by the addition of CN^- to form the mononuclear *trans*-chalcogenolato complex anions, *trans*-[bis(2-mercaptoethyl)methylaminato(2−)](cyanato)nickelate and *trans*-[bis(2-(hydroseleno)ethyl)methylaminato(2−)](cyanato)nickelate (Scheme 1). The results of single-crystal X-ray diffraction studies of the structures of the two dimers are summarized in Figures 1 and 2 and Tables 1−4. Figures 1 and 2 reveal that the structures of the compounds are strikingly similar, in keeping with the fact that the two crystalline solids are isomorphous (Table 1). The largest difference between the two structures is the 0.11 Å increase in the average Ni−chalcogen distance from $[Ni(\mathbf{1})]_2$ (average Ni−S = 2.183(4) Å) to $[Ni(\mathbf{2})]_2$ (average Ni−Se = 2.295(6) Å). The Ni centers in both compounds are best described as distorted planar complexes featuring one tertiary amine and three chalcogenolate donor atoms. The trans angles involving the N-donor atom show the greatest deviation from the ideal value of 180°. For $[Ni(\mathbf{1})]_2$, the trans S−Ni−S angles average 177.5(2)°, while the N−Ni−S angles have an average value of 165.6(3)°. The corresponding values for the Se−Ni−Se and N−Ni−Se angles in $[Ni(\mathbf{2})]_2$ are 175.6(2) and 166.8(9)°, respectively. Distortions from ideal geometry in the angles formed by cis ligand donor atoms are largest for the angles that involve the bridging chalcogen atoms. The ring angles at Ni average 82.6(1) and 83.2(2)°; the exocyclic angles average 97.4(2) and 95.7(3)° for $[Ni(\mathbf{1})]_2$ and $[Ni(\mathbf{2})]_2$, respectively.

The two planar Ni complexes in each molecule are joined along an edge via two bridging chalcogenolate donor atoms, leaving one terminal chalcogenolate ligand for each Ni atom. The molecules have no crystallographic symmetry but feature a pseudo-2-fold axis that relates the two Ni centers. The

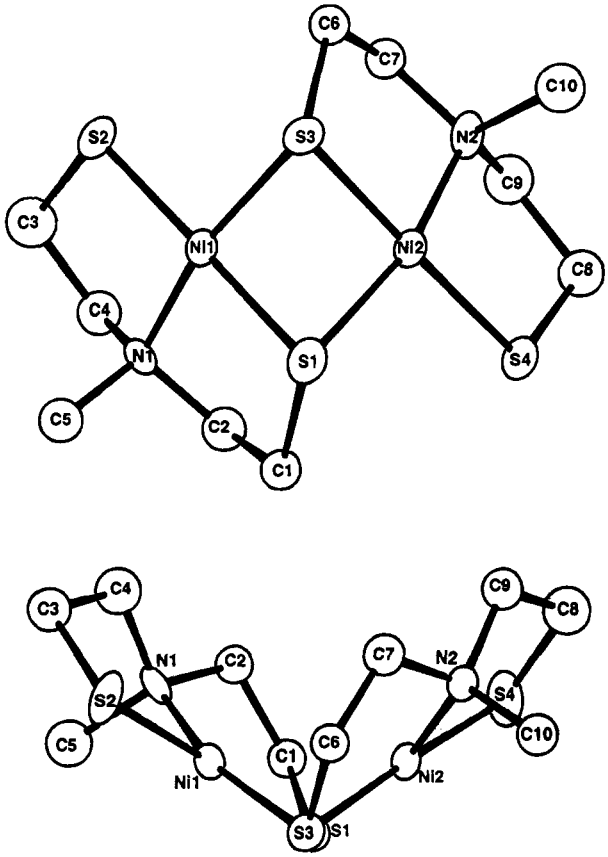

Figure 1. ORTEP plots of $[Ni(\mathbf{1})]_2$ with thermal ellipsoids at the 30% probability level: top, view normal to the plane defined by the vectors Ni1−Ni2 and S1−S2; bottom, view showing the fold along S1−S2. Hydrogen atoms are omitted for clarity.

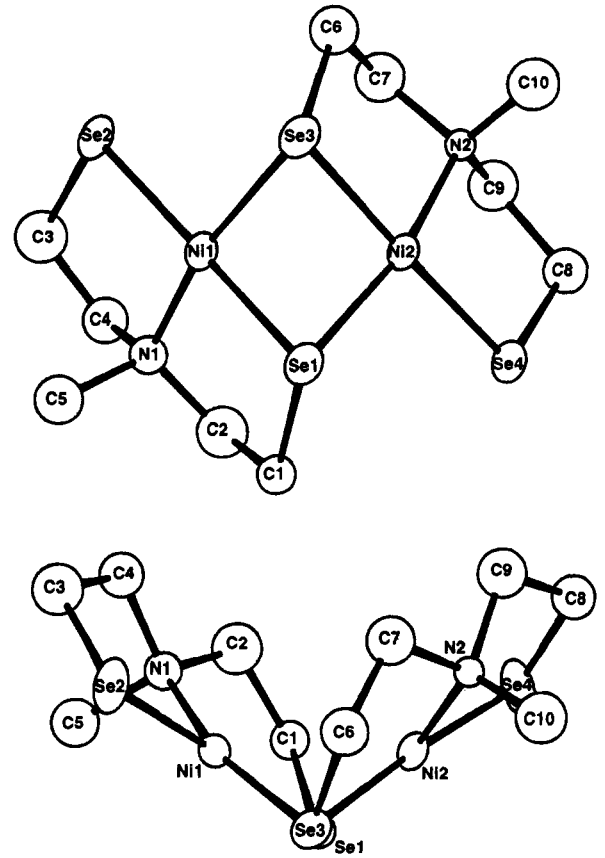

Figure 2. ORTEP plots of $[Ni(\mathbf{2})]_2$ with thermal ellipsoids at the 30% probability level: top, view normal to the plane defined by the vectors Ni1−Ni2 and Se1−Se2; bottom, view showing the fold along Se1−Se2. Hydrogen atoms are omitted for clarity.

idealized molecular symmetry is C_2; the small deviations observed from this symmetry are presumably due to packing. The bridging chalcogenolate ligands have the syn−endo conformation that is characteristic of such bridges when they are derived from chelating ligands.[18] The *N*-methyl groups of the tertiary amine donors have a syn−exo configuration, which is consistent with the C_2 symmetry of the molecules and distinguishes the structure of $[Ni(\mathbf{1})]_2$ from the closely related structure of a complex featuring pendant $-CH_2CH_2SMe$ N-substituents.[18]

In keeping with the syn−endo conformation, the central rhomb is not planar but is folded along a line connecting the bridging chalcogen atoms (Figures 1 and 2), which results in Ni−Ni distances of 2.679(2) and 2.722(6) Å for $[Ni(\mathbf{1})]_2$ and $[Ni(\mathbf{2})]_2$, respectively. The fold angle, defined as the dihedral angle between the planes formed by the Ni and the bridging chalcogen atoms, is 108.4(1)° in the thiolato complex and decreases to 103.6(2)° in the selenolato complex (Figures 1 and 2).

Spectroscopy and Redox Chemistry. The electronic absorption spectra of $[Ni(\mathbf{1})]_2$, $[Ni(\mathbf{2})]_2$, and their CN^- adducts are compared in Figure 3 and in Table 5. The spectrum of $[Ni(\mathbf{1})]_2$ features several poorly resolved bands in the 250 → 350 nm region of the spectrum. With the exception of the shoulders near 340 nm, these features are associated with RS^- → Ni charge transfer transitions.[13] The spectrum of $[Ni(\mathbf{2})]_2$ shows similar poorly resolved features, shifted to longer wavelength, with a maximum at 350 nm. The red shift is consistent with the increased polarizability of the selenolate ligands. The addition of 2 equiv of CN^- to $[Ni(\mathbf{1})]_2$ results in the formation of 2 equiv of a planar *trans*-dithiolato complex, $Et_4N[Ni(\mathbf{1})CN]$, where the CN^- ligands replace the bridging thiolates.[13] This complex has strong electronic absorptions near 275 and 310 nm. For $[Ni(\mathbf{2})]_2$, the addition of $Et_4N(CN)$ to a DMF solution results in very similar spectral changes; two new intense absorptions are observed near 280 and 327 nm. Again, the shift to longer wavelengths is consistent with the change in chalcogenide donor atom.

In addition to having electronic absorption spectra generally similar to those of the thiolato complexes, the selenolate complexes exhibit ^{77}Se-NMR spectra that confirm the nature of their structures. The NMR spectrum obtained from $[Ni(\mathbf{2})]_2$ reveals two peaks of equal intensity (δ = 204, −28 ppm), consistent with the retention of the dimeric structure in solution. The spectrum obtained from a solution of $Et_4N[Ni(\mathbf{2})CN]$ reveals a single resonance (δ = 150 ppm), consistent with the conversion of the dimer to a single mononuclear species, $[Ni(\mathbf{2})CN]^-$.

Exposure of a solution of $Et_4N[Ni(\mathbf{1})CN]$ to O_2 results in the conversion of one of the thiolate ligands to a sulfinate ligand with the incorporation of both atoms of dioxygen.[13,19] The electronic absorption spectrum observed for the monosulfinato product is also shown in Figure 3 and features shifts in the two maxima that are characteristic of the *trans*-dithiolato complex (to shorter (264 nm) and longer (325 nm) wavelengths, respectively). Spectra taken during the reaction are characterized by isosbestic points near 310 and 420 nm and have been used to measure the rate of the oxidation (rate = $k[Ni][O_2]$; k = 2.0×10^{-2} M^{-1} s^{-1} at 30 °C). The reaction has a $t_{1/2}$ = 1.8

(18) Colpas, G. J.; Kumar, M.; Day, R. O.; Maroney, M. J. *Inorg. Chem.* **1990**, *29*, 4779−88.

(19) Kumar, M.; Colpas, G. J.; Day, R. O.; Maroney, M. J. *J. Am. Chem. Soc.* **1989**, *111*, 8323−5.

Table 2. Selected Distances (Å) and Angles (deg) for $[Ni(\mathbf{1})]_2$ and $[Ni(\mathbf{2})]_2$[a]

	$[Ni(\mathbf{1})]_2$	$[Ni(\mathbf{2})]_2$
	Distances	
Ni1−S(Se)1	2.221(4)	2.327(5)
Ni1−S(Se)2	2.172(4)	2.263(5)
Ni1−S(Se)3	2.180(4)	2.303(5)
Ni2−S(Se)1	2.179(4)	2.287(7)
Ni2−S(Se)3	2.210(4)	2.343(7)
Ni2−S(Se)4	2.136(4)	2.247(7)
Ni1−N1	1.94(1)	1.92(3)
Ni2−N2	1.92(1)	1.96(2)
S(Se)1−C1	1.78(1)	1.97(4)
S(Se)2−C3	1.80(2)	2.02(5)
S(Se)3−C6	1.89(1)	2.02(4)
S(Se)4−C8	1.82(2)	1.90(4)
Ni1−Ni2	2.679(2)	2.722(6)
S(Se)1−S(Se)3	2.899(5)	3.074(6)
	Angles	
S(Se)1−Ni1−S(Se)2	177.3(2)	175.7(2)
S(Se)1−Ni1−S(Se)3	82.4(1)	83.2(2)
S(Se)2−Ni1−S(Se)3	98.2(1)	95.0(2)
S(Se)1−Ni1−N1	88.3(3)	90.0(8)
S(Se)2−Ni1−N1	91.7(3)	92.6(9)
S(Se)3−Ni1−N1	164.8(3)	166.0(9)
S(Se)3−Ni2−S(Se)4	177.7(2)	175.4(2)
S(Se)1−Ni2−S(Se)3	82.7(1)	83.2(2)
S(Se)1−Ni2−S(Se)4	96.6(2)	96.4(3)
S(Se)3−Ni2−N2	90.9(3)	90.1(8)
S(Se)1−Ni2−N2	90.3(3)	91.1(7)
S(Se)1−Ni2−N2	166.5(3)	167.5(8)
Ni1−S(Se)1−C1	75.0(1)	72.3(2)
Ni1−S(Se)1−C1	99.7(5)	96(1)
Ni2−S(Se)1−C1	113.0(5)	109(1)
Ni1−S(Se)2−C3	99.2(5)	92(1)
Ni1−S(Se)3−Ni2	75.2(1)	71.7(2)
Ni1−S(Se)3−C6	108.2(5)	108(1)
Ni2−S(Se)3−C6	95.7(5)	92(1)
Ni2−S(Se)4−C8	98.9(6)	94(1)
fold angle	108.4(1)	103.6(2)

[a] Estimated standard deviations in parentheses. Atoms are labeled to agree with Figures 1 and 2.

Table 3. Atomic Coordinates in Crystalline $[Ni(\mathbf{1})]_2$[a]

atom	x	y	z	B_{eq}[b] (Å^2)
Ni1	0.69275(7)	0.1612(3)	0.287	2.84(3)
Ni2	0.55682(7)	0.1613(3)	0.2795(2)	2.82(3)
S1	0.6203(2)	−0.0067(6)	0.3885(2)	3.53(8)
S2	0.7671(2)	0.3129(8)	0.1892(3)	4.68(9)
S3	0.6288(2)	0.0094(6)	0.1737(3)	3.91(8)
S4	0.4856(2)	0.2952(9)	0.3830(3)	4.9(1)
N1	0.7267(5)	0.325(2)	0.4006(8)	3.6(3)
N2	0.5203(5)	0.346(2)	0.1763(7)	2.7(2)
C1	0.6336(7)	0.153(2)	0.4983(9)	3.5(3)*
C2	0.6710(7)	0.366(3)	0.4710(9)	3.5(3)*
C3	0.8045(8)	0.507(2)	0.275(1)	4.6(3)*
C4	0.7547(9)	0.541(3)	0.363(1)	5.2(4)*
C5	0.7859(8)	0.192(3)	0.447(1)	5.3(4)*
C6	0.6149(8)	0.219(2)	0.071(1)	3.5(3)*
C7	0.5766(8)	0.415(3)	0.111(1)	4.2(3)*
C8	0.4453(8)	0.499(3)	0.302(1)	5.6(4)*
C9	0.4921(8)	0.555(3)	0.220(1)	4.2(3)*
C10	0.4701(8)	0.234(3)	0.111(1)	4.2(4)*

[a] Numbers in parentheses are estimated standard deviations. [b] Equivalent isotropic thermal parameters are calculated as $(4/3)[a^2\beta_{11} + b^2\beta_{22} + c^2\beta_{33} + ab(\cos\gamma)\beta_{12} + ac(\cos\beta)\beta_{13} + bc(\cos\alpha)\beta_{23}]$. Starred values are for atoms refined isotropically.

h at 30 °C under 1 atm of O_2 in DMF.[13] Reaction of $Et_4N[Ni(\mathbf{2})CN]$ with O_2 in DMF under identical conditions does not lead to a change in the electronic absorption spectrum like the one observed for the thiolato complex (Figure 3). In fact, over the period of time characteristic of the thiolate oxidation,

Table 4. Atomic Coordinates in Crystalline $[Ni(\mathbf{2})]_2$[a]

atom	x	y	z	B_{eq}[b] (Å^2)
Ni1	0.6910(2)	0.1506(6)	0.287	2.96(9)
Ni2	0.5554(2)	0.1521(6)	0.2767(5)	3.04(9)
Se1	0.6176(2)	−0.0299(5)	0.3901(3)	3.87(8)
Se2	0.7653(2)	0.3019(8)	0.1825(4)	5.2(1)
Se3	0.6286(2)	−0.0084(6)	0.1647(3)	4.12(9)
Se4	0.4801(2)	0.2824(7)	0.3836(4)	5.0(1)
N1	0.722(1)	0.315(4)	0.396(2)	3.5(6)*
N2	0.521(1)	0.336(4)	0.172(2)	2.2(5)*
C1	0.632(2)	0.153(6)	0.506(3)	3.7(8)*
C2	0.670(2)	0.357(7)	0.470(4)	6(1)*
C3	0.799(2)	0.503(6)	0.288(4)	7(1)*
C4	0.752(2)	0.526(6)	0.368(3)	5(1)*
C5	0.781(2)	0.196(6)	0.443(4)	6(1)*
C6	0.609(2)	0.214(6)	0.061(3)	6(1)*
C7	0.577(2)	0.410(7)	0.110(4)	6(1)*
C8	0.446(2)	0.488(5)	0.294(3)	4.9(9)*
C9	0.497(2)	0.547(6)	0.215(3)	6(1)*
C10	0.474(2)	0.242(7)	0.106(4)	7(1)*

[a] Numbers in parentheses are estimated standard deviations. [b] See footnote *b* of Table 3.

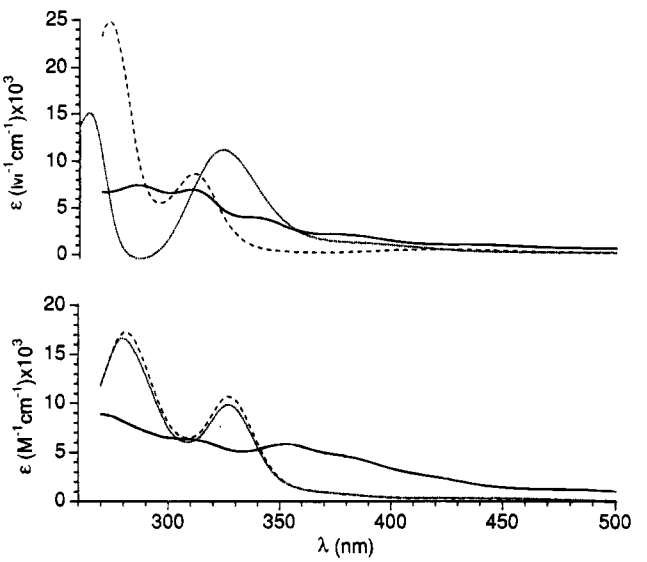

Figure 3. Electronic absorption spectra with extinction coefficients on a per Ni basis. Top: $[Ni(\mathbf{1})]_2$ in DMF (solid line), $[Ni(\mathbf{1})CN]^-$ in DMF (dashed line), and the oxidation product isolated after 6 h exposure to O_2, $[Ni(\mathbf{1}\text{-}O_2)CN]^-$ in acetonitrile (dotted line). Bottom: $[Ni(\mathbf{2})]_2$ in DMF (solid line), $[Ni(\mathbf{2})CN]^-$ in DMF (dashed line), and sample after exposure to O_2 for 6 h in DMF (dotted line).

Table 5. Electronic Absorption Spectroscopic Data

complex	solvent	λ (nm) (ϵ (M^{-1} cm^{-1}))	ref
$[Ni(\mathbf{1})]_2$	DMF	289 (6280), 312 (5970), 340 (sh), 376 (sh), 432 (sh), 552 (570)	13
$Et_4N[Ni(\mathbf{1})CN]$	DMF	275 (18 700), 312 (7530), 432 (661)	13
$[Ni(\mathbf{2})]_2$	DMF	273 (sh), 310 (6320), 353 (5790), 384 (sh), 420 (sh), 475 (sh)	this work
$Et_4N[Ni(\mathbf{2})CN]$	DMF	282 (22 900), 327 (14 100), 596 (24)	this work

little change in the spectrum of $[Ni(\mathbf{2})CN]^-$ is observed. Over an extended period of time (>4 days), the spectrum of $[Ni(\mathbf{2})CN]^-$ gradually decreases in intensity. Clearly, the selenolate complex is not oxidized to a dioxoselenium(II) species, in contrast with the chemistry that is observed for the thiolate complex.

The electrochemical studies of $[Ni(\mathbf{1})]_2$ and $[Ni(\mathbf{2})]_2$ are summarized in Figure 4 and Table 6. The electrochemistry of both complexes is characterized by irreversible processes, which

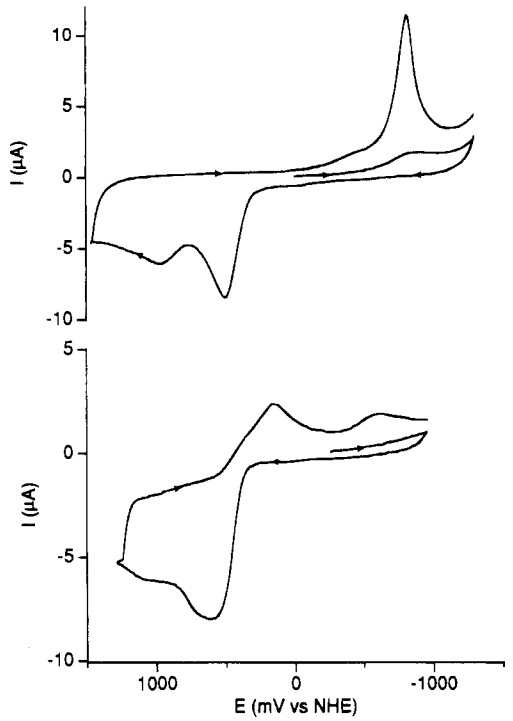

Figure 4. Cyclic voltammograms obtained from 1 mM solutions of $[Ni(1)]_2$ (top) and $[Ni(2)]_2$ (bottom) in 0.1 M n-$Bu_4N(ClO_4)/CH_2Cl_2$ solutions at a scan rate of 250 mV/s.

complicates the interpretation of the redox chemistry involved. When the initial potential scan is in the cathodic direction, no reduction of the thiolato-bridged dimer is observed within the limit of the solvent/electrolyte window (*ca.* −1.5 V vs NHE). Similarly, $[Ni(2)]_2$ exhibits a cathodic peak for an irreversible process only near the window limit ($Ep_c \sim 1.40$ V; not shown). Therefore, neither dimer is easily reduced. When the initial scan is in the anodic direction, $[Ni(1)]_2$ reveals an irreversible oxidation with $Ep_a = +490$ mV (scan rate = 250 mV/s). The corresponding oxidation for $[Ni(2)]_2$ occurs near +520 mV. Coulometric analysis reveals that both of these oxidations are one-electron processes, and both one-electron-oxidation products reveal $S = {}^1/_2$ EPR signals that integrate to one unpaired spin per dimer (*vide infra*). Scanning to greater anodic potentials reveals a second oxidation in each case. In the case of $[Ni(1)]_2$, the second oxidation (+960 mV) is coupled to the appearance of a new cathodic wave (−880 mV). For $[Ni(2)]_2$, there is evidence of a second oxidation near +1.0 V; however, the cathodic wave at +145 mV is coupled to the first oxidation. The second reduction at −630 mV more likely corresponds to the −880 mV reduction process from oxidized $[Ni(1)]_2$. It was not possible to perform a coulometric analysis of the second oxidation in either case, due to the formation of a film on the working electrode. The cyclic voltammograms do not change with scan rate over the range 100−1000 mV/s, other than to exhibit slight shifts in the peak potentials. Repeated cycling over the potential ranges indicated in Figure 4 did not lead to any change in the voltammogram obtained from either compound.

One-electron oxidation of the dimers results in the formation of $S = {}^1/_2$ radical cations, which are formulated as dimers, $[Ni(1)]_2^+$ and $[Ni(2)]_2^+$ (*vide infra*). The electronic structure of the oxidation products were probed using EPR spectroscopy. EPR spectra obtained from frozen CH_2Cl_2 solutions of $[Ni(1)]_2^+$ and $[Ni(2)]_2^+$ are compared in Figure 5 and Table 6. Each oxidation product reveals a rhombic EPR spectrum with very similar g values. It is possible to prepare samples of $[Ni(1)]_2^+$ either by bulk electrolysis or by chemical oxidation with $NO(BF_4)$. However, $[Ni(1)]_2^+$ and other analogous thiolato complexes[20] are thermally unstable and react to form EPR-silent products even at −40 °C, the lowest temperature that does not lead to the precipitation of the supporting electrolyte from 0.1M n-$Bu_4N(ClO_4)/CH_2Cl_2$ solutions. For this reason, samples prepared for EPR studies were rapidly oxidized to *ca.* 70%, transferred to EPR tubes, and frozen. These solutions exhibit a rhombic EPR signal ($g_x = 2.20$, $g_y = 2.14$, $g_z = 2.02$) that does not show any resolved hyperfine interaction arising from the N-donor ligand. Integration of the EPR signal obtained from these samples corresponded to 100 ± 10% the number of electrons involved in the electrolysis. For $[Ni(2)]_2$, electrolyses performed at −40 °C did not lead to the observation of a significant EPR signal. Thus, the selenolato radical appears to be less thermally stable than the thiolato complex. Samples for EPR studies of $[Ni(2)]_2^+$ were prepared at −70 °C via chemical oxidation with $NO(BF_4)$, transferred to cold EPR tubes, and frozen in liquid N_2 within a few minutes of preparation. Under these conditions, integration of the EPR signal accounts for the conversion of 96 ± 10% of the sample to a single oxidation product. Frozen solutions of $[Ni(2)]_2^+$ exhibit EPR spectra that differ only slightly from those observed for the thiolato analog ($g_x = 2.23$, $g_y = 2.14$, $g_z = 2.05$) (Figure 5). One difference in the two spectra is the observation of natural abundance ^{77}Se ($I = {}^1/_2$, 7.58%) in the $[Ni(2)]_2^+$ spectrum. This hyperfine interaction is resolved on the high-field (g_z) feature, which exhibits a single, large coupling, $A_z = 129$ G. Estimates of the magnitudes of the ^{77}Se hyperfine coupling constants were obtained from simulations of the EPR spectrum (Figure 5, Table 6). These simulations reveal an essentially axial hyperfine tensor, consistent with an unpaired electron in a $4p_z$ orbital, with $|A_{||}| = 129$ G and $|A_\perp| = 70.0$ G. Analysis of the ^{77}Se hyperfine coupling leads to an estimate of the spin density on Se of 54%, assuming equal participation of four Se-donor atoms in the molecular orbital containing the unpaired spin.[21]

Discussion

Structures. The structures obtained from isomorphous crystals of $[Ni(1)]_2$ (Figure 1) and $[Ni(2)]_2$ (Figure 2) are essentially the same, with the largest difference being the increase of 0.11 Å in the average Ni−chalcogenide bond length that accompanies the substitution of S by Se (Table 2). Thus, this pair of complexes constitutes an example of structurally analogous Ni alkanethiolato and alkaneselenolato complexes. The structures of both complexes are similar to those of other

(20) Pressler, M. A. Ph.D. Thesis, University of Massachusetts, 1993.

(21) The hyperfine coupling can be written as $A_z = A_{||} = a + 2T$ and ${}^1/_2(A_x + A_y) = A_\perp = a - T$, where a = the isotropic contact term and T = the anisotropic dipolar term (Wertz, J. E.; Bolton, J. R. *Electron Spin Resonance: Elementary Theory and Practical Applications*; McGraw-Hill: New York, 1972). An estimate of the unpaired electron density per Se atom was obtained by comparing the experimentally determined value of T with a theoretical value for one unpaired electron in a ^{77}Se 4p orbital, $T_0 = 492$ MHz (Hurd, C. M.; Coodin, P. *J. Phys Chem. Solids* **1967**, *28*, 523−5), $\varrho_{spin} \approx T/T_0$. The experimentally determined values of T and a depend on the relative signs of $A_{||}$ and $A_\perp$, information which cannot be obtained from a frozen-solution spectrum. Thus, T and a were calculated for two cases: (1) where $A_{||}$ and $A_\perp$ have the same sign and (2) where they have opposite signs. For the case where $A_{||}$ and $A_\perp$ have the same sign, values of $T = 19.6$ G and $a = 89.7$ G are obtained and lead to a value of $\varrho_{spin} = 0.040$/Se. For the case where $A_{||}$ and $A_\perp$ have opposite signs, values of $T = 66.3$ G and $a = 3.7$ G are obtained and lead to a value $\varrho = 0.135$/Se. The latter value provides an estimate of the Se character of the HOMO (54%), assuming equal contributions from four Se atoms. The latter values are favored over the lower estimate, on the basis of estimates of spin density at Ni obtained from a complex analogous to $[Ni(1)]_2$ and by analogy with formally Ni(III) diselenolene complexes (see Discussion).

Table 6. Electrochemical and EPR Spectroscopic Data

complex	E_{p_a} (mV vs NHE)	E_{p_c} (mV vs NHE)	n(first E_{p_a}) (E_{elec} (mV vs NHE))	EPR parameters	ref
$[Ni(\mathbf{1})]_2$	+490		0.81 (+650)	$g_{x,y,z}$ = 2.20, 2.14, 2.02	this work
	+960	−880			
$[Ni(\mathbf{2})]_2$	+610	+145	1.0 (+590)	experiment	this work
	+1000	−630		$g_{x,y,z}$ = 2.23, 2.14, 2.05	
				$^{77}SeA_z$ = 129 (exp)	
				simulation	
				$g_{x,y,z}$ = 2.216, 2.130, 2.044 (sim)	
				$^{77}SeA_{x,y,z}$ (G) = 70.0, 70.0, 129 (sim)	
$[Ni(tds)_2]^-$				$g_{x,y,z}$ = 2.188, 2.112, 2.006	32
				$^{77}SeA_{x,y,z}$ (G) = 61, 51, 190	
$[Ni(tfd)_2]^-$				$g_{x,y,z}$ = 2.137, 2.043, 1.996	32
$[Ni(mnt)_2]^-$				$g_{x,y,z}$ = 2.140, 2.043, 1.996	32
D. gigas—**C**		−270 (EPR appearance)		$g_{x,y,z}$ = 2.19, 2.14, 2.02	2, 3
T. roseopersicina—**C**				$g_{x,y,z}$ = 2.20, 2.14, 2.01	26
D. baculatus—**C**				$g_{x,y,z}$ = 2.20, 2.16, ~2.0	9

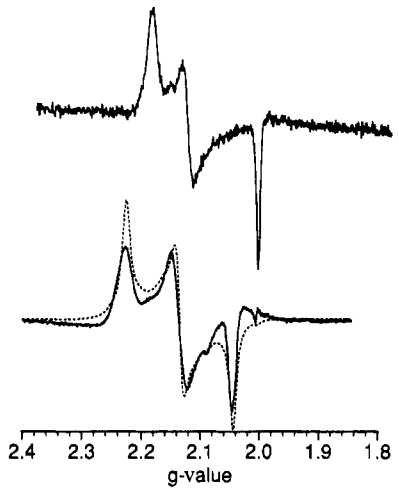

Figure 5. EPR spectra of the one-electron oxidation products $[Ni(\mathbf{1})]^{2+}$ (top) and $[Ni(\mathbf{2})]_2^+$ (bottom). The dashed line on the bottom figure is the simulated spectrum obtained with the g values (line widths in G) g_x = 2.216 (15.1), g_y = 2.130 (10.0), g_z = 2.044 (10.2) and hyperfine coupling constants (G) A_x = 70.0, A_y = 70.0, A_z = 129.

known dimeric complexes with dithiolato bridges, where the bridging S atoms are involved in chelate rings and have the expected syn−endo conformation.[18]

Another example of structurally analogous Ni(II) alkanethiolato and alkaneselenolato complexes that also feature Ni in planar coordination environments are the complexes obtained from 1,2-ethanedithiolate and 1,2-ethanediselenolate.[22] The average Ni−Se bond length observed for the bis(1,2-ethanediselenolate) complex is 2.305(3) Å. This value is indistinguishable from that observed for $[Ni(\mathbf{2})]_2$ (2.295(6) Å) and is also 0.11 Å longer than the average Ni−S distance observed in the bis(1,2-ethanedithiolate) complex.[23] The Ni−Se distances observed for $[Ni(\mathbf{2})]_2$ are also similar to those observed in planar Ni(II) complexes featuring bis(diselenolene) coordination (*e.g.* L = bis(trifluoromethyl)-1,2-ethanediselenolate, bis-tds, average Ni−Se = 2.255 Å;[24] L = *o*-benzenediselenolate, average Ni−Se = 2.259 Å[25]) but substantially shorter than those observed for tetrahedral (*e.g.* [Ni(dmp)(2,4,6-$Me_3C_6H_2Se)_2$],[26] average Ni−Se = 2.36 Å) or five-coordinate complexes (*e.g.* [Ni(terpy)-(2,4,6-$Me_3C_6H_2Se)_2$],[26] average Ni−Se = 2.42 Å).

The average Ni−S distance in $[Ni(\mathbf{1})]_2$ (2.18 Å) is comparable to Ni−S distances found in hydrogenases by EXAFS analysis (~2.2 Å),[26−28] although the Ni−Se distance for the Ni−Se−cys complex in *D. baculatus* H_2ase (2.44 Å)[8] is considerably longer than the distance observed in planar selenolate complexes. Thus, the bond lengths found in the enzymes are more consistent with a five- or six-coordinate Ni site in the enzyme. This is also in agreement with the Ni K-edge XAS analyses, which also indicate a five- or six-coordinate site in H_2ases.[27−29] Thus, $[Ni(\mathbf{1})]_2$ and $[Ni(\mathbf{2})]_2$ are poor structural models for the single Ni site in H_2ases. Nonetheless, their redox chemistry provides insights into the electronic structure of the Ni sites in H_2ases and a possible role for Se−cys ligation.

Chemistry and Spectroscopy. Prior studies of thiolato-bridged dimers confirm the retention of the dimeric structure in solution and the cleavage of these dimers upon addition of CN^-.[13,18,28,30] For the selenolate complex, the dimeric structure of $[Ni(\mathbf{2})]_2$ in solution and its cleavage in the presence of CN^- are supported by the ^{77}Se-NMR spectra and by the observation of electronic absorption spectra that are similar to those observed for structurally characterized thiolate analogs. Cyclic voltammetric studies of the dimers (Figure 4, Table 6) reveal that neither complex is easily reduced to complexes containing formal Ni(I) centers. However, both dimers may be oxidized by one electron to form cation radicals. The oxidation products are thermally unstable and react completely to form EPR-silent products in a few minutes at ambient temperatures.

Given the irreversible nature of the electrochemical processes, it is tempting to conclude that the oxidation products are no longer dimers. However, several facts suggest that the dimeric structure is retained upon oxidation. First, there is structural precedence for a dimeric structure. The formally Ni(III)/Ni(II) dimer obtained from one-electron oxidation of a Ni(II) complex of tris(*o*-mercaptophenyl)phosphine is a $S = {}^1/_2$ dimer and features the same core structure as $[Ni(\mathbf{1})]_2$.[31] Each Ni center

(22) Marganian, C. A.; Baidya, N.; Olmstead, M. M.; Mascharak, P. K. *Inorg. Chem.* **1992**, *31*, 2992−4.
(23) Baidya, N.; Mascharak, P. K.; Stephan, D. W.; Campagna, C. F. *Inorg. Chim. Acta* **1990**, *177*, 233−8.
(24) Heuer, W. B.; Squattrito, P. J.; Hoffman, B. M.; Ibers, J. A. *J. Am. Chem. Soc.* **1988**, *110*, 792−803.
(25) Sandman, D. J.; Allen, G. W.; Acampora, L. A.; Stark, J. C.; Jansen, S.; Jones, M. T.; Ashwell, G. J.; Foxman, B. M. *Inorg. Chem.* **1987**, *26*, 1664−9.
(26) Baidya, N.; Noll, B. C.; Olmstead, M. M.; Mascharak, P. K. *Inorg. Chem.* **1992**, *31*, 2999−3000.
(27) Bagyinka, C.; Whitehead, J. P.; Maroney, M. J. *J. Am. Chem. Soc.* **1993**, *115*, 3576−85.
(28) Colpas, G. J.; Maroney, M. J.; Bagyinka, C.; Kumar, M.; Willis, W. S.; Suib, S. L.; Mascharak, P. K.; Baidya, N. *Inorg. Chem.* **1991**, *30*, 920−8.
(29) Eidsness, M. K.; Sullivan, R. J.; Scott, R. A. In *The Bioinorganic Chemistry of Nickel*; Lancaster, J. R., Jr., Ed.; VCH: New York, 1988; pp 73−91.
(30) Kumar, M.; Day, R. O.; Colpas, G. J.; Maroney, M. J. *J. Am. Chem. Soc.* **1989**, *111*, 5974−6.
(31) Franolic, J. D.; Wang, W. Y.; Millar, M. *J. Am. Chem. Soc.* **1992**, *114*, 6587−8.

has a five-coordinate distorted pyramidal ligand environment composed of the two bridging S atoms, the P atom, and two terminal thiolato ligands. Second, repeated cycling over the potential ranges indicated in Figure 4 did not lead to any change in the voltammogram obtained from either $[Ni(\mathbf{1})]_2$ or $[Ni(\mathbf{2})]_2$. This indicates that the redox chemistry is chemically reversible on the cyclic voltammetric time scale, since nothing is consumed and no new products are formed. This observation is also consistent with the notion that the one-electron-oxidation products are still dimers. Cleavage of the dimer upon oxidation must form one mononuclear complex and one mononuclear radical in order to be consistent with the one-electron stoichiometry and would require rapid and complete recombination of the monomers upon reduction of the radical in order to be consistent with the absence of any new species (*e.g.* mononuclear complexes) and the lack of any loss of starting dimer. (The most likely dimerization, the coupling of two radicals, is not observed since it would give rise to a species that is not observed in terms of a new redox process or loss of starting material.) Third, a similar thiolato dimer differing only in the N-substituents, exhibits a quasi-reversible one-electron oxidation, and the oxidation product has the same voltammogram as that obtained from the starting material.[30] Fourth, the line broadening observed in the EPR spectra of radicals obtained from dimers similar to $[Ni(\mathbf{1})]_2$ and labeled with ^{61}Ni is best accounted for by a model involving coupling of the spin to two nearly equivalent Ni centers.[20,32] Given the close similarity of the spectra obtained from $[Ni(\mathbf{1})]_2^+$ and the selenolate analog, a dimeric structure is also expected for the one-electron-oxidation product of $[Ni(\mathbf{2})]_2$. It is likely that the irreversible nature of the one-electron oxidations observed for $[Ni(\mathbf{1})]_2$ and $[Ni(\mathbf{2})]_2$ arises from another structural change, such as coordination of the solvent, that accompanies oxidation of these dimers. The binding of additional ligands upon oxidation of Ni(II) to Ni(III) complexes is a common feature in many systems.[33,34]

The one-electron-oxidation products of $[Ni(\mathbf{1})]_2$ and $[Ni(\mathbf{2})]_2$ both exhibit rhombic EPR spectra arising from $S = {}^1/_2$ species (Figure 5, Table 6). The spectra are strikingly similar to those obtained from a catalytically viable redox state (form **C**) of H_2-ase (Table 6). In fact, the spectrum of $[Ni(\mathbf{1})]_2^+$ is the first compound that we are aware of that reproduces the g values of the EPR spectrum associated with H_2ase in form **C** within ± 0.01 (Table 6). The fact that the spectrum obtained from the selenolato complex is quite similar to that obtained from the thiolato complex is exactly what would have been expected on the basis of the comparison of spectra obtained from H_2ases containing Ni−Se−cys ligation (*e.g. D. Baculatus* H_2ase, Table 6). The spectrum of $[Ni(\mathbf{2})]_2$ also reveals hyperfine coupling arising from interaction of the spin with natural-abundance ^{77}Se nuclei. Analysis of the epr spectrum by the method employed by Maki and by Hoffman in formally Ni(III) dithiolene[35] and diselenolene[36] complexes using the magnitude of the hyperfine coupling estimated from simulations of the spectrum ($^{77Se}A_{x,y,z}$ (G) = 70.0, 70.0, 129) indicates that the orbital containing the spin is predominantly Se in character (54%). In fact, there appears to be little difference in the EPR spectra obtained from dithiolenes and diselenolenes as well as from these thiolate and selenolate complexes. Thus, the estimated spin density on Se in $[Ni(\mathbf{2})]_2^+$ is consistent with estimates obtained from a diselenolene complex[36] and also agrees with estimates of spin density on Ni (<30%) obtained from studies of ^{61}Ni-substituted dimers analogous to $[Ni(\mathbf{1})]_2$.[20,32]

The similarity between the EPR spectra obtained from $[Ni(\mathbf{1})]_2^+$ and $[Ni(\mathbf{2})]_2^+$ and those obtained from H_2ase and from formally Ni(III) dithiolenes and diselenolenes suggests either that EPR spectroscopy is a remarkably poor probe of electronic structure in these systems or that there are similar features in the electronic structures of all of these Ni centers. It is possible that the spectra reflect the fact that the electronic structures of these complexes are dominated by the M−chalcogenide interaction and that oxidation involves an orbital that is largely chalcogenide in character. In the case of the dithiolenes and diselenolenes, this view is supported by theoretical calculations[37,38] and by the lack of significant spin density on the ethylene C atoms.[36] Thus, oxidation of Ni(II) to Ni(III) in dithiolenes and diselenolenes is seen to involve an orbital that is mainly chalcogenide in character (50−65% (S), 70% (Se)[36]) and is not expected to be significantly different from the case of dithiolates and diselenolates that also form five-membered chelate rings. The possible involvement of a similar dithiolate interaction in the Ni site in H_2ase is indicated by the conservation of two Cys−X−X−Cys amino acid sequences in 17 H_2ases,[4] one of which is the site of the Se−cys substitution—the only Ni ligand to be specifically identified.[8] Such sequences could give rise to Ni complexes not unlike dithiolates and dithiolenes and are a likely explanation for the observation that the charge density on Ni does not change significantly during redox cycling of the enzyme.[39]

The difference in the reactivity of $[Ni(\mathbf{1})CN]^-$ and $[Ni(\mathbf{2})CN]^-$ with O_2 is in stark contrast to the general similarity of the chemistry of these complexes. Reaction of thiolato-bridged dimers like $[Ni(\mathbf{1})]_2$ with CN^- leads to the formation of mononuclear *trans*-dithiolato complexes, two of which have been structurally characterized.[13,19] This reaction is associated with the appearance of two intense absorptions in the UV spectrum (Figure 3, Table 5). In the case of $[Ni(\mathbf{1})CN]^-$, these bands appear at 275 and 312 nm. Similarly, reaction of $[Ni(\mathbf{2})]_2$ with CN^- leads to the formation of a complex with absorptions at 281 and 327 nm. The red shift observed for these two transitions is consistent with the replacement of S-donors by more polarizable Se-donor atoms. Reaction of $[Ni(\mathbf{1})CN]^-$ with 1 atm of O_2 at 30 °C proceeds with a half-life of 1.8 h and can be monitored by electronic absorption spectroscopy.[13] The spectra reveal isosbestic points near 310 and 420 nm associated with the conversion of the spectrum to that of the product, a monosulfinato complex, which absorbs at 264 and 325 nm in acetonitrile, a solvent where both bands may be observed (Figure 3). Similar oxidations have also been observed in a number of structurally unrelated Ni (II) thiolate complexes[40] and in Ni(II) bis(dithiolenes).[41] Reaction of $[Ni(\mathbf{2})CN]^-$ with O_2 under identical conditions does not lead to any immediate change in the spectrum of the complex. After 6 h (over 3 half-lives for the thiolato complex), a small decrease in the intensity of the

(32) Maroney, M. J.; Pressler, M. A.; Mirza, S. A.; Whitehead, J. P., Gurbiel, R. J.; Hoffman, B. M. In *Mechanistic Bioinorganic Chemistry*; Thorp, H., Pecoraro, V., Eds.; American Chemical Society: Washington, DC, 1994.
(33) Lappin, A. G.; McAuley, A. *Adv. Inorg. Chem.* **1988**, *32*, 241−94.
(34) Haines, R. I.; McAuley, A. *Coord. Chem. Rev.* **1981**, *39*, 77−119.
(35) Maki, A. H.; Edelstein, N.; Davison, A.; Holm, R. H. *J. Am. Chem. Soc.* **1964**, *86*, 4580−7.
(36) Heuer, W. B.; True, A. E.; Swepston, P. N.; Hoffman, B. M. *Inorg. Chem.* **1988**, *27*, 1474−82.
(37) Alvarez, S.; Vicente, R.; Hoffmann, R. *J. Am. Chem. Soc.* **1985**, *107*, 6253−77.
(38) Sano, M.; Adachi, H.; Yamatera, H. *Bull. Chem. Soc. Jpn.* **1981**, *54*, 2636−41.
(39) Whitehead, J. P.; Gurbiel, R. J.; Bagyinka, C.; Hoffman, B. M.; Maroney, M. J. *J. Am. Chem. Soc.* **1993**, *115*, 5629−35.
(40) Farmer, P. J.; Solouki, T.; Mills, D. K.; Soma, T.; Russell, D. H.; Reibenspies, J. H.; Darensbourg, M. Y. *J. Am. Chem. Soc.* **1992**, *114*, 4601−5.
(41) Schrauzer, G. N.; Zhang, C.; Chadha, R. *Inorg. Chem.* **1990**, *29*, 4104−7.

overall spectrum of [Ni(**2**)CN]$^-$ is observed (Figure 3), but no new bands or isosbestic points are formed. This decrease continues for several days. It is apparent that an O_2 oxidation similar to those that occur in Ni thiolate complexes does not occur in the selenolato complex.

Fe,Ni H_2ases are deactivated upon exposure to air in a process that is dependent on O_2 and results in a weak interaction of the $S = {}^1/_2$ center in the oxidized enzymes with $^{17}O_2$, suggesting that O_2 binds near the Ni site.[42] One possible mechanism for the deactivation of the enzyme by O_2 would involve the oxidation of a Ni cysteinate ligand in the enzyme to a cysteine sulfenate or sulfinate ligand. Several facts point to this possibility. First, there are two oxidized forms of the enzyme with distinct EPR signals (**A** and **B**) that also differ in their kinetics of reductive activation. Exposure to H_2 leads to the rapid reduction of form **B**, while form **A** exhibits a lag that has been associated with removal of O_2 from the sample.[2] Thus, form **A** could represent a form that has an oxidized Ni–cysteinate ligand. Evidence that supports this notion includes the fact that form **B** may be prepared anaerobically using alternative oxidants, while form **A** cannot. Furthermore, form **B** has been shown to react in air to produce form **A**. This reaction is slow, with $t_{1/2}$ on the order of several hours to days, depending on the enzyme and the temperature.[2] This time scale is similar to what is observed for the oxidation of [Ni(**1**)CN]$^-$ and similar thiolate complexes.[13] Last, the substitution of Se for the oxygen-sensitive S-donor atom might be expected to increase the oxygen tolerance of the enzyme, since oxides of Se are more difficult to form than S oxides and are more readily reduced.[43] This is clearly the case with respect to the reaction of [Ni(**2**)CN]$^-$ with O_2, which does not result in the formation of the oxidation product that is characteristic of the thiolate complexes. This also appears to be the case for *D. baculatus*, H_2ase, which can be isolated in air in an EPR-silent state without oxidation to form either **A** or **B**.[5] The chemistry presented here is consistent with an antioxidant role for Se in Fe,Ni,Se enzymes.

Acknowledgment. This research was supported by NIH Grant GM-38829 (M.J.M.).

Supplementary Material Available: Tables of anisotropic thermal parameters, distances and angles, and hydrogen atom parameters for [Ni(**1**)]$_2$ (Tables S1–S3) and for [Ni(**2**)]$_2$ (Tables S4–S6) (8 pages). Ordering information is given on any current masthead page.

(42) van der Zwaan, J. W.; Coremans, J. M. C. C.; Bouwens, E. C. M.; Albracht, S. P. J. *Biochim. Biophys. Acta* **1990**, *1041*, 101–10.

(43) Greenwood, N. N.; Earnshaw, A. *Chemistry of the Elements*; Pergamon Press: New York, 1984; pp 911–3.